Magnetic Neutron Diffraction from Exchange-Coupled Lattices at High Temperatures

M. SLOTNICK
Randall Physics Laboratories, University of Michigan, Ann Arbor, Michigan
(Received April 9, 1951)

The magnetic scattering of slow neutrons from a crystal lattice with exchange coupling at temperatures much higher than the (ferromagnetic or antiferromagnetic) Curie point is investigated. The residual short-range order is shown to manifest itself in coherent and inelastic effects, which are calculated by means of an expansion in $1/T$. These effects can yield information on the strength of the exchange interactions, the ratio of nearest neighbor to next nearest neighbor interactions, etc. Conditions for the observability of these effects are more favorable in the antiferromagnetic case.

I. INTRODUCTION

COHERENT effects in the magnetic scattering of neutrons from the antiferromagnetic substance MnO at room temperature were first observed by Shull and Smart.[1] Recently, more detailed experiments have been performed on MnO by Bendt and Rainwater.[2] Since MnO has a Curie temperature of 122°K, the scattering effects constitute one of the very few detectable effects of exchange coupling at temperatures far above the Curie point. It was therefore thought of interest to make a detailed theoretical calculation of the magnetic neutron diffraction pattern in this temperature region, particularly since here the rigorous high temperature expansion methods are available and make possible relatively unequivocal statements. These enable one, at least in principle, to obtain from the experimentally observed pattern a considerable amount of information on the exchange interaction strengths, etc.

In Sec. II, the specifically coherent scattering effects are investigated for a lattice with nearest neighbor and next nearest neighbor exchange coupling, for both the ferromagnetic and antiferromagnetic cases. In Sec. III, several inelastic effects neglected in Sec. III are taken into account.

II. THE COHERENT MAGNETIC SCATTERING

The magnetic scattering of slow neutrons (i.e., that part of the scattering due to the interaction of the neutron magnetic moment with the electronic magnetic moments) has been studied by Halpern and Johnson[3] and many others. They found that for neutrons of momentum $\mathbf{k}$ and spin s incident on a lattice in a state L, the ratio of measured intensity of neutrons of momentum $\mathbf{k}'$ and spin s' in a solid angle range $d\Omega$ to incident neutron intensity is

$$di=(2e^2\mu_N/m)^2|(s'L'|\textstyle\sum_n(\mathbf{s}\cdot\mathbf{S}_n-\mathbf{q}^*\cdot\mathbf{s}\mathbf{q}^*\cdot\mathbf{S}_n)\times\exp(-\mathbf{q}\cdot\mathbf{R}_n)|sL)|^2F(q)d\Omega. \quad (1)$$

Here L' is the final lattice state, m is the electronic mass, μ_n is the magnetic moment of the neutron, $\mathbf{s}$ is the neutron spin operator, $\mathbf{S}_n$ and $\mathbf{R}_n$ are the spin operator and position respectively of the nth ion, and the sum is over all N ions in the lattice. Further, $\hbar$ and c have been taken as unity and

$$\mathbf{q}=\mathbf{k}'-\mathbf{k};\quad \mathbf{q}^*=\mathbf{q}/|\mathbf{q}|, \quad (2)$$

and

$$F^{\frac{1}{2}}(q)=\mathcal{S}^{-1}(B|\exp(-\mathbf{q}\cdot\mathbf{r}_l)\mathbf{s}_l\cdot\mathbf{S}|B)\quad(\mathcal{S}\equiv S(S+1)) \quad (3)$$

is the magnetic form factor of the individual ion, B being the state of the individual ion, $\mathbf{s}_l$ and $\mathbf{r}_l$ the spin and location of its lth electron, and $\mathbf{S}$ its total spin.

It has been assumed that the orbital magnetic interactions are absent or quenched, and that the neutrons are being detected with an efficiency inversely proportional to the velocity, so that a $|\mathbf{k}'|/|\mathbf{k}|$ term is absent in (1). We assume also that the region of observation is far from a nuclear Bragg peak, so that there is no interference with nuclear scattering. The nuclear scattering may then simply be subtracted from the total measured scattering to give the magnetic scattering.

Of experimental interest is the total intensity of scattered neutrons in a given direction $\mathbf{k}^{*\prime}=\mathbf{k}'/|\mathbf{k}'|$. If we therefore sum (1) over all possible final states for which $\mathbf{k}'$ lies in the specified direction, and average over the initial neutron spin states (assuming an unpolarized beam) we obtain for the ratio of intensity in the direction $\mathbf{k}^{*\prime}$ (per unit solid angle) to incident neutron intensity:

$$I(\mathbf{k},\mathbf{k}^{*\prime})=\sum_L Z^{-1}\exp(-E_L/T)\sum_{\text{ad }L'}(e^2\mu_N/m)^2F(q)\cdot|(L'|\textstyle\sum_n(\mathbf{S}_n-\mathbf{q}^*\mathbf{q}^*\cdot\mathbf{S}_n)\exp(-i\mathbf{q}\cdot\mathbf{R}_n)|L)|^2. \quad (4)$$

Here $Z^{-1}\exp(-E_L/T)$ is the probability of occupation of the lattice state L, where

$$Z(T)=\textstyle\sum_L\exp(-E_L/T). \quad (5)$$

(T measured in energy units) and E_L is the exchange energy of the state L, which we take to be the eigenfunction of a hamiltonian

$$H=J\sum_{\text{nbr }l,l'}\mathbf{S}_l\cdot\mathbf{S}_{l'}+K\sum_{n\text{ nbr }l,l'}\mathbf{S}_l\cdot\mathbf{S}_{l'}. \quad (6)$$

The specifications "nbr l, l'" and "n nbr l, l'" refer to

[1] C. J. Shull and J. S. Smart, Phys. Rev. **76**, 1256 (1949).
[2] P. J. Bendt and L. J. Rainwater, Phys. Rev. **83**, 235 (1951).
[3] O. Halpern and M. H. Johnson, Phys. Rev. **55**, 898 (1939).

the fact that the first sum is taken over all ions l and l' that are nearest neighbors, the second over all l and l' that are next nearest neighbors. J and K are proportional to certain exchange integrals and are positive in the antiferromagnetic, negative in the ferromagnetic case. The instruction "ad L'" in the sum over final states in (4) means that only those final lattice states with admissible energies are to be included. That is, the kinetic energy of the scattered neutron

$$k'^2/(2M)=k^2/(2M)+E_L-E_{L'} \tag{7}$$

must be $\geqslant 0$, or $E_{L'}\leqslant E_L+k^2/(2M)$. ($M$ is the neutron mass.)

To proceed with the evaluation of (4), two approximations are made, which will be examined more closely in Sec. III. First, we assume that in the admissible transitions, $\mathbf{q}$ is seldom very far from its value $\mathbf{q}_0$ for a purely elastic transition:

$$q_0=2k\sin\tfrac{1}{2}\vartheta;\quad |\mathbf{k}'|=|\mathbf{k}|, \tag{8}$$

where ϑ is the angle between $\mathbf{k}$ and $\mathbf{k}'$. We thus substitute $\mathbf{q}_0$ for $\mathbf{q}$ in the matrix element of (4) and in the argument of the form factor. Second, we assume that the final lattice states L' to which a nonzero matrix element exists in (4) are almost all energetically accessible, so that in the summation over final states, we may sum over all states to which a nonzero matrix element exists. The first approximation depends on q being fairly large compared to the rms energy change, the second on k being fairly large.

$I(\mathbf{k},\mathbf{k}^{*\prime})$ then becomes (with $\mathbf{R}_{nn'}$ written for $\mathbf{R}_n-\mathbf{R}_{n'}$)

$$\begin{aligned}I(\mathbf{k},\mathbf{k}^{*\prime})&=(e^2\mu_N/m)^2F(q_0)Z^{-1}\textstyle\sum_L\exp(-E_L/T)\\&\quad(L|\textstyle\sum_{nn'}(\mathbf{S}_n-\mathbf{q}^*{}_0\mathbf{q}^*{}_0\cdot\mathbf{S}_n)\cdot(\mathbf{S}_{n'}-\mathbf{q}^*{}_0\mathbf{q}^*{}_0\cdot\mathbf{S}_{n'})\\&\quad\times\exp(i\mathbf{q}_0\cdot\mathbf{R}_{nn'})|L)\\&=(e^2\mu_N/m)^2F(q_0)Z^{-1}\\&\quad\times\mathrm{Sp}\{\textstyle\sum_{nn'}(\mathbf{S}_n\cdot\mathbf{S}_{n'}-\mathbf{q}_0{}^*\cdot\mathbf{S}_n\mathbf{q}_0{}^*\cdot\mathbf{S}_{n'})\\&\qquad\times\exp(i\mathbf{q}_0\cdot\mathbf{R}_{nn'})\exp(-H/T)\}.\end{aligned} \tag{9}$$

Next, the $\exp(-H/T)$ is expanded:

$$\exp(-H/T)=\sum_{m=0}^{\infty}(-1)^m/m!(H/T)^m$$

in both the argument of the spur in (9) and in

$$Z(T)=\textstyle\sum_L(L|\exp(-H/T)|L)=\mathrm{Sp}\exp(-H/T), \tag{10}$$

and a series is obtained for $I(\mathbf{k},\mathbf{k}^{*\prime})$:

$$I(\mathbf{k},\mathbf{k}^{*\prime})=I_0+T^{-1}I_1+T^{-2}I_2+\cdots. \tag{11}$$

To terms in $1/T^2$,

$$Z(T)=(2S+1)^N\{1+T^{-2}(N\mathcal{S}^2/3)(J^2z_n+K^2z_{nn})\} \tag{12}$$

where z_n and z_{nn} are the numbers of nearest and next nearest neighbors respectively of a given lattice point. It is characteristic that because of the factor N, the number of ions in (12)—the expansion for Z, an extensive property of the lattice, is in powers of $(N^{\frac{1}{3}}/T)$, and is thus extraordinarily poor at laboratory temperatures. The series for $I(\mathbf{k},\mathbf{k}^{*\prime})$, however, is in powers of $1/T$, and is usable at ordinary temperatures. (In all of these calculations, frequent use is made of the following formulas for taking spurs:

$$\begin{aligned}&\mathrm{Sp}'S_\mu=0\\&\mathrm{Sp}'S_\mu S_\nu=\mathcal{S}/3\delta_{\mu\nu}\\&\mathrm{Sp}'S_\mu S_\nu S_\kappa=i/6\mathcal{S}e_{\mu\nu\kappa}\\&\mathrm{Sp}'S_\kappa S_\lambda S_\mu S_\nu=\mathcal{S}/30[(2\mathcal{S}+1)(\delta_{\kappa\lambda}\delta_{\mu\nu}+\delta_{\kappa\nu}\delta_{\mu\lambda})\\&\qquad\qquad+(2\mathcal{S}-4)\delta_{\kappa\mu}\delta_{\lambda\nu}],\end{aligned}$$

where $e_{\mu\nu\kappa}$ is the permutation symbol, S_μ is the μ-component of a spin vector whose square is $S(S+1)\equiv\mathcal{S}$, and Sp′ indicates the spur divided by the number of states.) Further, it is found that

$$I_0(q_0)=(e^2\mu_N/m)^2F(q_0)\cdot\tfrac{2}{3}N\mathcal{S}, \tag{13}$$

which is the ordinary incoherent paramagnetic scattering (see reference 3) and

$$\begin{aligned}I_1(\mathbf{k},\mathbf{k}^{*\prime})&=(e^2\mu_N/m)^2F(q_0)\cdot\tfrac{2}{3}N\mathcal{S}\cdot(-\tfrac{2}{3}\mathcal{S})\\&\quad\times\{J\textstyle\sum_1\cos(\mathbf{q}_0\cdot\mathbf{R}_{ll'})+K\sum_2\cos(\mathbf{q}_0\cdot\mathbf{R}_{ll'})\},\end{aligned} \tag{14}$$

where $\sum_1$ is taken over all nearest neighbors l' of a single given lattice point l, and $\sum_2$ is over next nearest neighbors l' of l.

Actually, most experiments are performed with a microcrystalline powder, so that a typical lattice vector $\mathbf{R}_{ll'}$ will on the average be randomly located with respect to $\mathbf{q}_0$. We must, therefore, replace $\cos(\mathbf{q}_0\cdot\mathbf{R}_{ll'})$ by its average over-all directions of $\mathbf{R}_{ll'}$, which is

$$(q_0R_{ll'})^{-1}\sin(q_0R_{ll'}).$$

(14) then becomes (I_1 depends now only on k and the angle ϑ)

$$\begin{aligned}I_1(k,\vartheta)&=I_0(q_0)\cdot(-\tfrac{2}{3}\mathcal{S})\\&\quad\times\left\{Jz_n\frac{\sin q_0\Delta_n}{q_0\Delta_n}+Kz_{nn}\frac{\sin q_0\Delta_{nn}}{q_0\Delta_{nn}}\right\}\end{aligned} \tag{15}$$

where Δ_n and Δ_{nn} are the spacings between nearest and next nearest neighbors on the lattice respectively.

Note that to this approximation, the effects of nearest and next nearest neighbor interactions are completely additive—as are indeed the effects of any other interactions that may be present. This contrasts strongly with the situation below the Curie point, where the ordered lattice state may be determined by just one of the interactions.[4] In fact, it is possible by comparing the experimental location of the maxima or minima of the magnetic scattering pattern with those of (15) to infer the ratio of J to K, which can be used to check the theory of Anderson.[4]

[4] P. Anderson, Phys. Rev. **79**, 705 (1950).

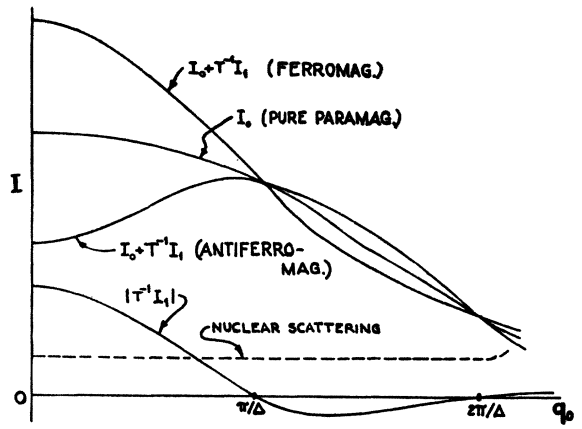

FIG. 1. Magnetic neutron scattering intensity per unit solid angle per unit incident beam (I) as function of $q_0=2k\sin\frac{1}{2}\vartheta$.

The relation between the ferro- and antiferromagnetic pattern is shown schematically in Fig. 1, where for simplicity we have assumed only one interaction, and plotted the intensity as functions of q_0. $I_0(q_0)$ [Eq. (13)], is just the form-factor pattern for an uncoupled paramagnetic lattice. The next term in the intensity, I_1 [Eq. (15)] is seen to be negative for the antiferromagnetic, positive for the ferromagnetic pattern, and is a coherent effect of the exchange coupling. In the ferromagnetic case, its principal effect is to increase the scattering for small q_0. This is difficult to observe first because of experimental difficulties at small q_0 (i.e., small angle or small neutron momentum k), and second because the inelastic effects to be discussed in Sec. III are very large in this region. The antiferromagnetic pattern, however, shows a coherent peak in the neighborhood of $q_0=\pi/\Delta$, and is readily observed. The inelastic effects, in fact, decrease the cross section at small q_0 and make the peak even more pronounced. The antiferromagnetic case is, therefore, much more accessible to experimental observation.

The antiferromagnetic coherent peak is the high temperature residue of the large coherent peak visible below the Curie temperature.[1] By examining the calculation of I_1, it is seen that the coherent effect arises from the correlation of ions directly coupled by an interaction [see Eq. (14)], and is thus an effect of the residual short-range order at high temperatures. It is in fact easy to compute the lowest order term in the temperature expansion for the average correlation of two ions at positions a and b in the lattice. The result is:

$$\langle(L|S_\alpha^{(a)}S_\beta^{(b)}|L)\rangle_{Av}=\tfrac{1}{3}\mathcal{S}\delta_{\alpha\beta}(-2J\mathcal{S}/3T)^{n_{ab}}s_{ab}, \quad (16)$$

where α and β refer to components of the spins of ions a and b, K has been assumed zero, n_{ab} is the minimum number of steps between a and b, counting distance between two neighbors as one step, and s_{ab} is the number of "shortest paths" between a and b, i.e., the number of ways of reaching b from a going from lattice point to lattice point, in precisely n_{ab} steps.

From (16), it is seen that the high temperature expansion is certainly poor at $T\lesssim 2|J|\mathcal{S}/3$, where the lowest order terms (16) indicate long-range order. The parameter $2J\mathcal{S}/(3T)$ is thus at high temperatures an indication of the degree of order, and is probably of the order of magnitude of unity at the Curie point.

The result for I_2 is, after some computation,

$$\begin{aligned}I_2=I_0\{&J^2[-\tfrac{1}{3}\mathcal{S}\textstyle\sum_1\cos\mathbf{q}_0\cdot\mathbf{R}_{ll'}+(4/9)\mathcal{S}^2\sum_{1'}\cos\mathbf{q}_0\cdot\mathbf{R}_{ll'}]\\&+K^2[-\tfrac{1}{3}\mathcal{S}\textstyle\sum_2\cos\mathbf{q}_0\cdot\mathbf{R}_{ll'}+(4/9)\mathcal{S}^2\sum_{2'}\cos\mathbf{q}_0\cdot\mathbf{R}_{ll'}]\\&+JK\cdot(8/9)\mathcal{S}^2\textstyle\sum_3\cos\mathbf{q}_0\cdot\mathbf{R}_{ll'}\}, \quad (17)\end{aligned}$$

where $\sum_1$ and $\sum_2$ have been defined above [Eq. (14)]. $\sum_{1'}$ is taken over all l' defined as follows: Pick any nearest neighbor of a given lattice site l. Then every nearest neighbor of this nearest neighbor, except l itself is taken as an l' in the sum. $\sum_{2'}$ is defined similarly—for "nearest neighbor" merely read "next nearest neighbor." In $\sum_3$, l' can be either a next nearest neighbor of a nearest neighbor of l, or the nearest neighbor of a next nearest neighbor.

After averaging over orientations of the microcrystals, (17) becomes

$$\begin{aligned}I_2=I_0\Big\{&J^2\Big[-\frac{1}{3}\mathcal{S}z_n\frac{\sin q_0\Delta_n}{q_0\Delta_n}+\frac{4}{9}\mathcal{S}^2z_n\sum_\alpha\omega_\alpha^{(1)}\frac{\sin q_0D_\alpha^{(1)}}{q_0D_\alpha^{(1)}}\Big]\\&+K^2\Big[-\frac{1}{3}\mathcal{S}z_{nn}\frac{\sin q_0\Delta_{nn}}{q_0\Delta_{nn}}+\frac{4}{9}\mathcal{S}^2z_{nn}\sum_\alpha\omega_\alpha^{(2)}\frac{\sin q_0D_\alpha^{(2)}}{q_0D_\alpha^{(2)}}\Big]\\&+JK\cdot\frac{8}{9}\mathcal{S}^2z_nz_{nn}\sum_\alpha\omega_\alpha^{(3)}\frac{\sin q_0D_\alpha^{(3)}}{q_0D_\alpha^{(3)}}\Big\}. \quad (18)\end{aligned}$$

Table I gives the $\omega_\alpha^{(i)}$, $D_\alpha^{(i)}$, etc., for several lattice types. It is not difficult to extend the results to other lattice types and to include other interactions. For each interaction, a term of the structure of the J^2 term in (17) must be included, and a cross-term like the JK term in (17) for every pair of interactions. To this order, there are no cross-terms involving more than two interactions.

III. INELASTIC EFFECTS

The approximations made in going from Eq. (4) for $I(\mathbf{k},\mathbf{k}^{*\prime})$ to Eq. (9) have led us to the expressions (11), (13), (15), and (18). These expressions are functions only of $q_0=2k\sin\frac{1}{2}\vartheta$, instead of both k and ϑ, so that if (as in the experiments of reference 2) $I(k,\vartheta)$ is measured as a function of k for several fixed angles $\vartheta_1,\vartheta_2,\cdots$ and the curves are plotted with q_0 as abscissa (as in Fig. 1), the curves taken at angles ϑ_1, ϑ_2, etc., should all coincide. We shall show now that if we take into account the neglected effects, the intensities are reduced somewhat (particularly for small q_0). Moreover, the curves for large ϑ are further depressed than those

TABLE I. Coefficients for Eq. (18).

Lattice type	$\frac{\Delta_{nn}}{\Delta_n}$	z_n	z_{nn}	i	$\omega_1^{(i)}$	$D_1^{(i)}$	$\omega_2^{(i)}$	$D_2^{(i)}$	$\omega_3^{(i)}$	$D_3^{(i)}$	$\omega_4^{(i)}$	$D_4^{(i)}$
Simple cubic	$\sqrt{2}$	6	12	1	4	$\sqrt{2}\Delta_n$	1	$2\Delta_n$				
				2	4	$\sqrt{2}\Delta_n$	2	$2\Delta_n$	4	$\sqrt{6}\Delta_n$	1	$\sqrt{8}\Delta_n$
				3	$\frac{2}{3}$	Δ_n	$\frac{2}{3}$	$\sqrt{3}\Delta_n$	$\frac{2}{3}$	$\sqrt{5}\Delta_n$		
Body-centered cubic	$\sqrt{2}$	8	6	1	3	Δ_{nn}	3	$\sqrt{2}\Delta_{nn}$	1	$\sqrt{3}\Delta_{nn}$		
				2	4	$\sqrt{2}\Delta_{nn}$	1	$2\Delta_{nn}$				
				3	1	$\frac{\sqrt{3}}{2}\Delta_{nn}$	1	$\frac{\sqrt{11}}{2}\Delta_{nn}$				
Face-centered cubic	$\sqrt{2}$	12	6	1	4	$\frac{\sqrt{2}}{2}\Delta_{nn}$	2	Δ_{nn}	4	$\frac{\sqrt{6}}{2}\Delta_{nn}$	1	$\sqrt{2}\Delta_{nn}$
				2	4	$\sqrt{2}\Delta_{nn}$	1	$2\Delta_{nn}$				
				3	$\frac{2}{3}$	$\frac{\sqrt{2}}{2}\Delta_{nn}$	$\frac{2}{3}$	$\frac{\sqrt{6}}{2}\Delta_{nn}$	$\frac{2}{3}$	$\frac{\sqrt{10}}{2}\Delta_{nn}$		

for smaller ϑ, so that the curves for ϑ_1, $\vartheta_2\cdots$ are actually separated. Otherwise, the results of Sec. II are not seriously modified.

We examine first the effect of having included in Eq. (9) transitions to a few states that would require the neutron to transfer more than its total kinetic energy to the lattice. To this end, we must compute the distribution of energy losses in the transitions admitted in Eq. (9), and decrease our computed intensity by the fraction of energetically inaccessible transitions. It will prove practicable to calculate only the lowest few moments of the energy loss distribution, and the shape of the entire curve will be inferred from these. In fact, since the entire effect is generally not very large, it will be sufficient to assume that the distribution is gaussian, with suitably fitted mean energy loss and rms energy loss.

The mean energy loss of the neutron, $\bar{\epsilon}(\mathbf{k}, \mathbf{k}^{*\prime})$ is obtained by inserting a factor $(E_{L'}-E_L)$ into the summand of Eq. (4), and dividing by the total intensity $I(\mathbf{k}, \mathbf{k}^{*\prime})$. (Note that for this purpose it is essential to sum over all states L', including the inaccessible, in both numerator and denominator.) We assume then that in the matrix element and the form factor, $\mathbf{q}$ may still be replaced with sufficient accuracy by $\mathbf{q}_0$. This yields:

$$\bar{\epsilon}(\mathbf{k}, \mathbf{k}^{*\prime})=\frac{\mathrm{Sp}\{\sum_{nn'}\exp(-i\mathbf{q}_0\cdot\mathbf{R}_{nn'})(\mathbf{S}_{n'}-\mathbf{q}^*_0\mathbf{q}^*_0\cdot\mathbf{S}_{n'})\cdot[H, (\mathbf{S}_n-\mathbf{q}^*_0\mathbf{q}^*_0\cdot\mathbf{S}_n)]\exp(-H/T)\}}{\mathrm{Sp}\{\sum_{nn'}\exp(-i\mathbf{q}_0\cdot\mathbf{R}_{nn'})(\mathbf{S}_{n'}-\mathbf{q}^*_0\mathbf{q}^*_0\cdot\mathbf{S}_{n'})\cdot(\mathbf{S}_n-\mathbf{q}^*_0\mathbf{q}^*_0\cdot\mathbf{S}_n)\exp(-H/T)\}} \tag{19}$$

where $[A, B]=AB-BA$. Expanding the $\exp(-H/T)$ and using the result

$$[H, \mathbf{S}_n]=-2Ji\sum_{\substack{\text{nbrs}\\ n' \text{ of } n}}\mathbf{S}_{n'}\times\mathbf{S}_n-2Ki\sum_{\substack{n \text{ nbrs}\\ n' \text{ of } n}}\mathbf{S}_{n'}\times\mathbf{S}_n \tag{20}$$

we find that $\bar{\epsilon}$ approaches zero at high temperatures. The lowest nonvanishing term in the high temperature expansion is (after performing the microcrystalline averaging)

$$\bar{\epsilon}(k, \vartheta)=+4\mathcal{S}/(3T)\left\{J^2z_n\left(1-\frac{\sin q_0\Delta_n}{q_0\Delta_n}\right)+K^2z_{nn}\left(1-\frac{\sin q_0\Delta_{nn}}{q_0\Delta_{nn}}\right)\right\} \tag{21}$$

indicating that the neutron tends to lose rather than gain energy at the lower temperatures. To this order, the interactions contribute additively to (21).*

To obtain the mean square neutron energy loss $\langle\epsilon^2(\mathbf{k}, \mathbf{k}^{*\prime})\rangle_{\mathrm{Av}}$, one proceeds identically, inserting, however, a factor $(E_{L'}-E_L)^2$ rather than $(E_{L'}-E_L)$ in Eq. (4). One finds for $\langle\epsilon^2\rangle_{\mathrm{Av}}$ an equation identical to (19), except that $[H, (\mathbf{S}_n-\mathbf{q}^*_0\mathbf{q}^*_0\cdot\mathbf{S}_n)]$ is replaced by

$$[H, [H, (\mathbf{S}_n-\mathbf{q}^*_0\mathbf{q}^*_0\cdot\mathbf{S}_n)]].$$

The lowest term in the high temperature expansion is then found to be

$$\langle\epsilon^2(k, \vartheta)\rangle_{\mathrm{Av}}=\frac{8\mathcal{S}}{3}\left\{J^2z_n\left(1-\frac{\sin q_0\Delta_n}{q_0\Delta_n}\right)+K^2z_{nn}\left(1-\frac{\sin q_0\Delta_{nn}}{q_0\Delta_{nn}}\right)\right\}. \tag{22}$$

This is temperature-independent, the interactions again contributing additively, and reduces for large $q_0\Delta_n$ and $K=0$ to an analogous result obtained by Van Vleck.[5]

* Including inaccessible states in the sum limits the use of (21) to neutrons of kinetic energy large compared to T. In general, (21) gives an upper limit to the magnitude of the neutron mean energy loss.

[5] J. H. Van Vleck, Phys. Rev. 55, 924 (1939), Eq. (7). Note in this connection that if it is desired to express the results in terms of magnetic susceptibility data [as in Eqs. (9) (10) of the reference], the expression $\Theta=\frac{2}{3}\mathcal{S}(Jz_n+Kz_{nn})$ should be used for the constant Θ in the susceptibility law $\chi=C(T+\Theta)^{-1}$. Comparing (18) and (15) shows that rapid convergence of (11) depends on the smallness of Θ/T. This must be remembered in applications to substances such as MnO for which Θ is much larger than the Curie temperature.

The probability that a neutron loses energy between ϵ and $\epsilon+d\epsilon$ in the scattering process is then taken to be

$$P(\epsilon)d\epsilon=(2\pi\langle\epsilon^2\rangle_{Av})^{-\frac{1}{2}}\exp\{-(\epsilon-\bar{\epsilon})^2/2\langle\epsilon^2\rangle_{Av}\} \quad (23)$$

so that since transitions for which $\epsilon>k^2/2M$ are prohibited, the previously determined intensity must be multiplied by the factor

$$\gamma(k,\vartheta)=1-\int_{k^2/2M}^{\infty}P(\epsilon)d\epsilon$$
$$=\tfrac{1}{2}[1+\Phi((k^2-2M\bar{\epsilon})/(8M^2\langle\epsilon^2\rangle_{Av})^{\frac{1}{2}})] \quad (24)$$

where Φ is the error function.[6] Note that $\gamma(k,\vartheta)$ depends on k and ϑ, not merely on q_0, so that the intensity curves for 2 different values of ϑ and varying k, will be separated. Since $k^2/2M=(8M\sin^2\frac{1}{2}\vartheta)^{-1}q_0^2$, it is seen from (24) that γ is larger for larger ϑ ($\bar{\epsilon}$ and $\langle\epsilon^2\rangle_{Av}$ depend only on q_0). $\gamma(k,\vartheta)$ is slightly greater than $\frac{1}{2}$ at $q_0=0$, rises fairly rapidly, and is rather close to unity in the region of antiferromagnetic coherent peak.

The second effect we consider is that of having replaced $\mathbf{q}$ by $\mathbf{q}_0$ in the form-factor in Eq. (4). Since the values of ϑ of interest are not too large (below the angle of the first Debye-Scherrer ring), q will be larger than q_0 for most transitions, whether the neutron gains or loses energy. Since the form-factor decreases monotonically with q, we exaggerate the intensity by replacing q by q_0, the exaggeration being worse, for given q_0, for larger ϑ.

To correct for this effect, we note that in the region of interest the form factor can be expressed sufficiently accurately as

$$F(q)\approx 1-\alpha q^2. \quad (25)$$

Furthermore, if the energy change is not too large compared to the initial neutron energy, we have using Eq. (7)

$$q^2=k^2+k'^2-2kk'\cos\vartheta\approx q_0^2+4M(E_L-E_{L'})\sin\tfrac{1}{2}\vartheta$$
$$+(1/k^2)M^2(E_L-E_{L'})^2\cos\vartheta. \quad (26)$$

Inserting (26) and (25) into (4), replacing $\mathbf{q}$ by $\mathbf{q}_0$ elsewhere in (4), and neglecting the effect of the energetically inaccessible states, $I(k,\vartheta)$ takes the form

$$I(k,\vartheta)=I_0(q_0)+T^{-1}I_1(q_0)+T^{-2}I_2(q_0)+\cdots$$
$$+\delta I_{FF}(k,\vartheta) \quad (27)$$

where I_0, I_1, and I_2 are given in (13), (15), and (18).

[6] Notation of Magnus and Oberhettinger, *Special Functions* (Chelsea Publishing Company, New York, 1949), p. 96.

For δI_{FF} we obtain, because of the factors $(E_L-E_{L'})$ and $(E_L-E_{L'})^2$ in (26), expressions much like the numerator of (19), etc. These may be evaluated by expansion of $\exp(-H/T)$ and give to lowest order the temperature-independent term

$$\delta I_{FF}(k,\vartheta)=-(e^2\mu_N/m)^2(\tfrac{2}{3}N\mathcal{S})((32/3)\alpha\mathcal{S}M^2\sin^2\tfrac{1}{2}\vartheta\cos\vartheta)$$
$$\cdot(J^2z_n\Delta_n^2R(q_0\Delta_n)+K^2z_{nn}\Delta_n^2R(q_0\Delta_{nn})) \quad (28)$$

where $R(x)=x^{-2}(1-x^{-1}\sin x)$ is a monotonically decreasing function of x, which is $\frac{1}{6}$ at $x=0$ and is again not very large in the region of interest.

Lastly we examine the effect of having replaced $\mathbf{q}$ by $\mathbf{q}_0$ in $\exp(-i\mathbf{q}\cdot\mathbf{R}_n)$ in Eq. (4). To this end we put

$$\exp(-i\mathbf{q}\cdot\mathbf{R}_n)\approx\exp(-i\mathbf{q}_0\cdot\mathbf{R}_n)(1-i\delta\mathbf{q}\cdot\mathbf{R}_n-\tfrac{1}{2}(\delta\mathbf{q}\cdot\mathbf{R}_n)^2)$$

where using (7)

$$\delta\mathbf{q}\equiv\mathbf{q}-\mathbf{q}_0=(k'-k)\mathbf{k}^{*\prime}\approx(Mk^{-1}(E_L-E_{L'})$$
$$-M^2k^{-3}(E_L-E_{L'})^2). \quad (29)$$

This results, after a somewhat tedious microcrystalline averaging, using methods similar to these used in the previous two calculations, in the addition to Eq. (27) of a term

$$\delta I_{\exp}(k,\vartheta)=-(e^2\mu_N/m)^2\cdot 8F(q_0)\cdot(1/9)\mathcal{S}^2N\cdot k^{-2}M^2$$
$$\cdot\{J^2z_n\Delta_n^2G(q_0\Delta_n)+K^2z_{nn}\Delta_{nn}^2G(q_0\Delta_{nn})\}, \quad (30)$$

where $G(x)=x^{-1}d/dx\,(x^{-1}\sin x)$.

Equation (3) is the first term in a high temperature expansion, and in its evaluation, $\mathbf{q}$ was replaced by $\mathbf{q}_0$ except in the exponential, and again the loss of energetically inaccessible transitions was neglected. Equation (30) is not reliable for very small q_0, since (29) is inaccurate there, but the effect is quite negligible in this region, and is in fact nowhere very large.

To recapitulate, the intensity pattern computed in Sec. II must be corrected by the term δI_{FF} [Eq. (28)] as in Eq. (27), and to this must be added the term $\delta I_{\exp}$ [Eq. (30)]. Finally, the resulting expression must be multiplied by the factor γ [Eq. (24)] to correct for the inclusion of energetically inaccessible transitions. These corrections may be observed directly experimentally as a separation in the $I(k,\vartheta)$ *vs* q_0 curves for 2 different ϑ and varying k, and may be employed as a further check on the values of J and K deduced from the strength and location of the antiferromagnetic coherent peak.

The author would like to thank Professor L. J. Rainwater and Dr. P. Bendt for stimulating this research, and for many useful discussions.